Published in final edited form as:
Neuroimage. 2010 October 15; 53(1): 247–256. doi:10.1016/j.neuroimage.2010.05.067.

Abnormal functional connectivity of default mode sub-networks in autism spectrum disorder patients

Michal Assaf[a,b,*], **Kanchana Jagannathan**[a], **Vince D. Calhoun**[a,b,c,d], **Laura Miller**[a], **Michael C. Stevens**[a,b], **Robert Sahl**[e], **Jacqueline G. O'Boyle**[a], **Robert T. Schultz**[f,g], and **Godfrey D. Pearlson**[a,b]

[a]Olin Neuropsychiatry Research Center, Institute of Living, Hartford Hospital, Hartford, CT, USA

[b]Department of Psychiatry, Yale University School of Medicine, New Haven, CT, USA

[c]The Mind Research Network, Albuquerque, NM, USA

[d]Department of Electrical and Computer Engineering, The University of New Mexico, Albuquerque, NM, USA

[e]Child and Adolescent Division, Institute of Living, Hartford Hospital, Hartford, CT, USA

[f]Center for Autism Research, Children's Hospital of Philadelphia, USA

[g]Department of Pediatrics, University of Pennsylvania School of Medicine, Philadelphia, PA, USA

Abstract

Autism spectrum disorders (ASDs) are characterized by deficits in social and communication processes. Recent data suggest that altered functional connectivity (FC), i.e. synchronous brain activity, might contribute to these deficits. Of specific interest is the FC integrity of the default mode network (DMN), a network active during passive resting states and cognitive processes related to social deficits seen in ASD, e.g. Theory of Mind. We investigated the role of altered FC of default mode sub-networks (DM-SNs) in 16 patients with high-functioning ASD compared to 16 matched healthy controls of short resting fMRI scans using independent component analysis (ICA). ICA is a multivariate data-driven approach that identifies temporally coherent networks, providing a natural measure of FC. Results show that compared to controls, patients showed decreased FC between the precuneus and medial prefrontal cortex/anterior cingulate cortex, DMN core areas, and other DM-SNs areas. FC magnitude in these regions inversely correlated with the severity of patients' social and communication deficits as measured by the Autism Diagnostic Observational Schedule and the Social Responsiveness Scale. Importantly, supplemental analyses suggest that these results were independent of treatment status. These results support the hypothesis that DM-SNs under-connectivity contributes to the core deficits seen in ASD. Moreover, these data provide further support for the use of data-driven analysis with resting-state data for illuminating neural systems that differ between groups. This approach seems especially well suited for populations where compliance with and performance of active tasks might be a challenge, as it requires minimal cooperation.

*Corresponding author. Olin Neuropsychiatry Research Center, Institute of Living, 200 Retreat Ave., Hartford, CT 06106, USA. Fax: +1 860 545 7797. massaf@harthosp.org (M. Assaf).

Appendix A. Supplementary data

Supplementary data associated with this article can be found, in the online version, at doi:10.1016/j.neuroimage.2010.05.067.

Keywords

Independent component analysis; Functional MRI; Resting state; Default mode network; High-functioning autism

Introduction

Autism spectrum disorders (ASDs) are neurodevelopmental conditions characterized by core deficits in social communication skills. One cognitive theory proposed to explain ASDs' deficits is that patients with ASD have difficulty with “Theory of Mind” (ToM) processes (Baron-Cohen, 1995; Hill and Frith, 2003). ToM is the ability to attribute states of mind (e.g. emotions, desires and goals) to other people and is a crucial component of social behavior. A distinct neural network normally mediates ToM, that includes medial prefrontal cortex (MPFC), temporoparietal junction, and temporal pole (Frith and Frith, 2003). A few studies have explored activation and functional connectivity of this network in individuals with ASDs using tasks of mental state attribution (Baron-Cohen et al., 1999; Castelli et al., 2002; Kana et al., 2009; Piggot et al., 2004) and narrative comprehension (Happé et al., 1996; Mason et al., 2008), with inconclusive results regarding the brain areas involved and the directionality of the impaired activation in relation to healthy controls.

Current research on social cognition in ASDs, including ToM, is limited to tasks that employ highly demanding cognitive procedures. This confines research to high-functioning and older subjects. Moreover, since patients' performance on these tasks is typically impaired, it is hard to conclude whether abnormal brain activations are primary, or secondary to patients' disengagement in the task. Studying brain networks that are activated during rest and overlap those related to social cognition, such as the default mode network (DMN), might overcome these limitations.

The DMN consists of the MPFC, posterior cingulate cortex/ retrosplenial cortex (PCC/Rsp) including the precuneus (PrC) and bilateral inferior parietal lobules (IPL) and systematically shows more prominent activity during passive resting conditions (e.g. Broyd et al., 2009; Buckner et al., 2008; Raichle et al., 2001). However, it is also active in tasks involving autobiographical memory, future prospection and ToM (for reviews see Broyd et al., 2009; Buckner et al., 2008). The close relationship between DMN and ToM network's brain areas makes it logical to explore whether abnormal DMN activity and/or functional connectivity might be related to ASD symptoms. The term “functional connectivity” (FC) refers to synchronous activation of spatially remote brain regions (Broyd et al., 2009; Friston et al., 1993; van de Ven et al., 2004). It has been suggested that functional under-connectivity among brain regions might explain ASD symptoms (Just et al., 2004). Several neuroimaging studies demonstrated reduced autism FC during the performance of different cognitive tasks (Castelli et al., 2002; Just et al., 2007, 2004; Kana et al., 2006, [2009], [2007]; Kleinhans et al., 2008; Koshino et al., 2005, 2008; Mason et al., 2008; Mostofsky et al., 2009; Solomon et al., 2009); although see other studies (Lee et al., 2008; Mizuno et al., 2006; Turner et al., 2006) for contradictory results.

Most studies investigating the DMN in individuals with ASDs analyzed data from resting blocks, comparing them to interleaved blocks of cognitive tasks, essentially measuring task induced deactiva-tions (TID) (Cherkassky et al., 2006; Kennedy and Courchesne, 2008a; Kennedy et al., 2006) and not FC per se (although Cherkassky et al. (2006) also performed a FC analysis, see below). Of those, Kennedy and Courchesne (2008a) and (Kennedy et al. 2006) showed abnormal DMN TID in patients. Measuring FC with a seed-voxel approach,Cherkassky et al. (2006) reported reduced anterior/posterior DMN connectivity in

ASD. However, resting block designs from cognitive tasks have limitations. First, patient cooperation and task understanding is required. Second, there is typically a correlation between DMN TID and task difficulty (e.g. McKiernan et al., 2003). Thus task difficulty in addition to task performance might influence group differences in DMN activations and connectivity.

To mitigate these drawbacks, subjects can be fMRI scanned during the resting state, where participants are instructed to lie still and awake in the scanner for few minutes, without performing any specific task. These scans are appealing to research involving patients because of their shortness and simplicity (Franco et al., 2009; Pearlson and Calhoun, 2009). While traditional analytical techniques such as the general linear model (GLM) using performance variables as regressors cannot be applied to resting data, it is possible to measure FC of different brain areas. To our knowledge, only two fMRI studies to date have tested resting state connectivity in ASD (Kennedy and Courchesne, 2008b; Monk et al., 2009). These calculated DMN connectivity within the network and with the rest of the brain, using a region of interest (ROI) seed-voxel correlation technique. *A priori* ROIs were defined based on previous reported DMN brain areas in healthy individuals. While both studies found decreased connectivity within the DMN, specifically involving the MPFC, Monk et al. (2009) also found increased connectivity between PCC and temporal regions in ASD. They further demonstrated that worse social functions in patients were associated with decreased connectivity between PCC and MPFC and that increased restrictive and repetitive behaviors were related to increased connectivity between PCC and parahippocampal gyrus. These results support impaired functional DMN connectivity as potentially underlying deficits seen in patients with ASD.

Group independent component analysis, ICA, has been recently used successfully to identify the DMN and other resting-state networks and to assess FC within these networks during resting fMRI scans (Calhoun et al., 2001b; McKeown and Sejnowski, 1998). ICA identifies spatially independent components of brain areas with hemodynamic timecourses that closely co-vary. Thus, the regions comprising each component are conceptualized as part of a specific network (Calhoun et al., 2001b) with highly synchronous time courses. ICA is a data-driven method, allowing data analysis without either regressors extracted from behavioral data (i.e. no task is needed) or *a priori* hypotheses of a specified relevant ROI. Thus, ICA identifies multiple integrated networks from fMRI timeseries data without being limited to *a priori* ROIs or specific cognitive processes (for review see Calhoun et al., 2009). It consistently identifies the DMN during scans of resting state and cognitive tasks in healthy individuals (e.g. Calhoun et al., 2008a; Stevens et al., 2009) and in patient groups (e.g. Garrity et al., 2007; Kim et al., 2009). Moreover, various ICA analyses suggest that resting fMRI data comprise several consistent synchronous networks, including fronto-parietal, motor, visual and auditory networks (Beckmann et al., 2005; Calhoun et al., 2008a; De Luca et al., 2006; Stevens et al., 2009; van de Ven et al., 2004). ICA has been used to identify sub-networks of the DMN as separate components, each with a distinctive timecourse. When detected in active tasks, all these sub-networks are negatively modulated by cognitive demands and include portions of typical DMN brain regions, namely MPFC and PCC/PrC (Beckmann et al., 2005; Calhoun et al., 2008a; Kim et al., 2009; Stevens et al., 2009). While seed-voxel correlation techniques can also detect DMN subnetworks (Uddin et al., 2009), ICA has the advantage of identifying sub-networks with subtly different spatiotemporal patterns, without specific ROI restriction. Thus, we used ICA to investigate the FC integrity of the default mode sub-networks (DM-SNs) during fMRI resting scans in high-functioning patients with ASD. We hypothesized that compared to matched healthy controls (HC), patients would show decreased strength of connectivity in DM-SNs, specifically in the PCC/PrC and MPFC (Broyd et al., 2009), and that social and communication skill deficits would be predicted by reduced connectivity within DM-SNs'.

Methods and materials

Participants

Sixteen high-functioning patients with ASDs (ages 11–20, 15 males) and 16 typically developing healthy controls (HC) (ages 13– 23, 14 males) were recruited. Full scale IQ was assessed with the Vocabulary and Block Design subsets of the Wechsler Adult Intelligence Scale (WAIS) or Wechsler Intelligence Scale for Children (WISC). Data from all 32 participants were used to run the ICA analysis and identify the DM-SNs. However, since IQ was missing for one patient and one control they were excluded from group analyses. Table 1 summarizes the demographic information for the remaining participants. Notably, there were no group differences on age, gender, race and full scale IQ. Patients' diagnosis was confirmed with the Autism Diagnostic Observational Schedule (ADOS, Lord et al., 2000) and the Autism Diagnostic Interview-Revised (ADI-R, Lord et al., 1994). ASD symptomatology was further assessed by the Social Responsiveness Scale (SRS, Constantino and Gruber, 2005), in the 13 patients younger than 18. Eight of the 15 patients were medicated when scanned (information was missing for 2 patients): 6 received CNS stimulants, 3 antipsychotic drugs, 4 SSRIs, 2 other antidepres-sants and one anti-epileptic treatment (note that 7 of the medicated patients were treated with more than one drug). ASD was ruled out in HCs using the ADOS (available for 14 of the 15 controls), the Social Communication Questionnaire (SCQ, Rutter et al., 2003) lifetime form (available for 9 controls, including the individual without ADOS) and a detailed health questionnaire. ADOS total scores ranged from 0 to 4 (mean=0.8±1.2) and SCQ scores ranged from 0 to 7 (mean=2.7± 2.9), well within the normal range. All participants provided written informed consent, approved by the Hartford Hospital Institution Review Committee, after complete description of the study and were paid for their time.

Scanning procedures

During fMRI, participants were instructed to lie still with their eyes open, fixating on a centrally presented cross for 5 minutes and 15 seconds. No cognitive task was performed during this time. Blood oxygenation level dependent (BOLD) signal was obtained with T2*-weighted echo planar imaging (EPI) sequence (TR/TE=1500/27 ms, Flip angle=70°, Field of view=22 cm with a 64×64 acquisition matrix) using a Siemens 3 T Allegra. We acquired 29 contiguous axial functional slices of 4 mm thickness with 1 mm gap, yielding 3.4×3.4×5 mm^3 voxels for 210 time points. The first 6 images of the scan were not included in the data analysis to allow global image intensity to reach equilibrium.

Image preprocessing

Data were preprocessed using SPM5 (Wellcome Department of Cognitive Neurology). Each individual's dataset was realigned to the first “non-dummy” image using the INRIAlign toolbox (A. Roche, INRIA Sophia Antipolis, EPIDAURE Group). The average translation motion parameter was 3.2 mm with no group differences ($t_{(1, 30)}$= 0.97, p=0.34). In addition to excluding components that represented movement artifacts (see below), all individual component maps were inspected to ensure that there were no obvious motion artifacts in the components of interest. Next, slice timing correction was applied to the data, adjusting slice timing based on the middle slice. Data were then spatially normalized to Montreal Neurological Institute (MNI) space (Friston et al., 1995), and smoothed with 9 mm^3 FWHM Gaussian kernel.

Component identification

Group spatial ICA was conducted for all 32 participants using the Infomax algorithm (Bell and Sejnowski, 1995) within the GIFT software (http://icatb.sourceforge.net/, version 1.3e).

Dimensionality estimation to determine the number of components was performed using the minimum description length criteria, modified to account for spatial correlation (Li et al., 2007). The mean dimension estimation was 28.9 (SD=13.4). We rounded this number slightly and estimated 28 components. Single subject time courses and spatial maps were then computed, during which the aggregate components and the results from data reduction were used to compute the individual subject components (i.e. back-reconstruction Calhoun et al., 2001a, 2009).

Selecting the components related to the DMN was done in 2 stages. First, a systematic process was used to inspect and select components whose patterns of correlated signal change were largely constrained to gray matter from the 28 estimated components (Stevens et al., 2007). To do so, the correlationsof each component's spatial map with *a priori* mask maps of gray matter, white matter, and cerebral spinal fluid (CSF) within standardized brain space provided in WFU Pickatlas (Maldjian et al., 2003) were computed. Components with high correlation to *a priori* localized CSF or white matter, or with low correlation to gray matter, were inferred to be likely artifactual. Visual inspection of discarded components suggested that they represented eye movements, head motion, or cardiac-induced pulsatile artifact at the base of the brain. Ten components were selected as of interest for further analysis to identify the DMN components.

Next, a spatial correlation analysis between the 10 chosen components and an a priori DMN binary mask of the DMN template provided in GIFT was performed. This template is based on DMN regions reported by Raichle et al. (2001), including the PCC/PrC, IPL and MPFC (Calhoun et al., 2008a,b; Garrity et al., 2007). This procedure was used only to select the components that corresponded to the DMN but not to modify them (i.e. no ROIs were included or excluded from the different components following this correlation analysis). Visual inspection confirmed that components that included all or part of the DMN regions ranked highest in this analysis.

For each subject, the chosen DMN components (3 components were chosen, see below), referred to here as the DM-SNs, were then converted to *z* values. For each component, individual maps of all subjects regardless of group were entered into random effect one-sample *t*-tests in SPM5 and thresholded at $p<0.05$ corrected for family-wise error, to create a sample-specific component map. These maps were used as a mask for group analyses within the corresponding component. Thus, results are not biased by components maps defined from healthy participants only.

Statistical analysis

Group comparison—Individual DM-SN components GIFT maps were entered into SPM5 for group analyses. The *z* values in these individual maps represent the fit of a specific voxel BOLD timecourse to the group averaged component's timecourse. Thus, group analyses test the connectivity strength (i.e. signal synchronization) of each voxel to the whole spatial component. For each component, random effects one-sample *t*-tests were performed for each group separately to assess the within group integrity of the component maps. Random effects two-sample *t*-tests examined group differences. The resulting statistical maps were masked with the study-specific general map of the relevant component (generated based on data from all participants) to explore results within this network only. All group tests were controlled for age and IQ (due to their wide range, see Table 1) and were thresholded at $p<0.05$ corrected for false discovery rate (FDR). Reported coordinates were converted from MNI space to standardized Talairach coordinates (Talairach and Tournoux, 1988) (http:// imaging.mrc-cbu.cam.ac.uk/imaging/MniTalairach).

To further assess the potential effect of drug treatment on results of group differences in functional connectivity, we recalculated the random effects two-sample *t*-test for each component, comparing only the 5 patients without current treatment to controls. In addition, for each component we performed random effects two-sample *t*-test comparing the patients without current treatment to the patients with current treatment (n=8; as mentioned above the treatment status of 2 patients was missing, therefore they were not included in these analyses). All group tests were controlled for age and IQ and were thresholded a $p<0.005$ uncorrected (due to the low number of subjects).

Correlation of components maps with symptom severity—For each DM-SN component, multiple regression analyses were performed to assess the relationship between individual patients' maps and their symptom severity as assessed by the ADOS total, communication and social scores and the SRS total and subscale scores. Again, analyses were controlled for age and IQ and thresholded at $p_{FDR}<0.05$, and the resulting statistical maps were masked with the general specific component's map, limiting the analysis to each component's ROIs.

Results

Component identification

Examination of the 10 component maps yielded 3 components that included brain areas previously reported to be part of the DMN (e.g. Broyd et al., 2009; Buckner et al., 2008; McKiernan et al., 2003; Raichle et al., 2001) (Fig. 1 and Table 2): (A) DMN component, including mainly the PCC and bilateral IPL, but also the PrC and MPFC (we refer to this network as the DMN since it is the only one that includes all suggested “classic” DMN regions); (B) Precuneus (PrC) component, which also included adjacent areas in the PCC, postcentral gyrus and paracentral lobule; and (C) MPFC component that also included a PCC/PrC cluster and small IPL clusters. Spatial correlation with the DMN *a priori* mask revealed that these components were the 3 highest ranking components of the 10 components of interest (r=0.30, 0.32 and 0.21 respectively), indicating that regions in these components closely resembled the regions in the mask. As evident in Fig. 1, some of the component maps partially overlap. One of the strengths of ICA is that a given voxel can contribute to multiple components. This provides for the case where a region can be a hub for more than one network (McKeown and Sejnowski, 1998).

One-sample *t*-tests that quantified conservation of spatial structure across participants in each component in each group separately demonstrated that the same brain regions were evident in the 3 selected ICA components in both groups (Table 2).

Group comparison

Although the DM-SNs' maps of patients and controls were similar overall, voxelwise two-sample *t*-tests revealed significant differences in regional FC strength for component A in the precuneus (x=21, y= –56, z=38; t=4.7, $p_{FDR}<0.05$), and for component C in the ACC (x= –9, y=47, z=–2; t=4.65, $p_{FDR}<0.05$). For both components patients showed decreased strength of connectivity compared to HC (Fig. 2).

Analyses including only patients with no current drug treatment replicated these results, showing stronger connectivity in HC in the precuneus (x=15, y=–53, z=38, t=3.86) for component A and in the ACC (χ=–9, y=49, z=–2, t=3.58) for component C. In our a priori threshold of p<0.005, additional group differences were found in the PCC (x=–3, y=–40, 13, t=3.43) in component A, and in the right ACC (χ=6, y=47, z=0, t=3.98) in component C (as in the original results, patients showed decreased strength of connectivity compared to HC).

In addition, comparing drug-treated patients to non-treated patients found no group differences in any of the 3 components.

Importantly, we used data from all participants regardless of diagnostic group to identify components, and to test for group differences in the second-level analyses, to avoid the problem of matching components between groups. This approach preserves group differences in the back-reconstructed maps (Calhoun et al., 2001a,b). We also performed a separate ICA for each group and identified the 3 DM-SNs components in both groups. Follow-up 2 sample *t*-tests found regional group differences similar to the group differences describe above (see Supplementary Materials).

Correlation of DM-SNs' connectivity maps with symptoms severity

Component A: No correlations were found with ADOS and SRS scores ($p_{FDR}<0.05$).

Component B: Significant negative correlations were found between the precuneus FC strength and ADOS total and social scale scores (x=0, y=−42, z=44, r=−0.90 and r=−0.89, respectively, $p_{FDR}<0.05$) and ADOS communication scale score (x=0, y=−41, z=63, r=−0.85, $p_{FDR}<0.05$) while controlling for age and IQ. The correlation pattern indicates that worse symptom severity was associated with lesser PrC connectivity (Fig. 3; Note that graphs depict participants with and without drug treatment at the time of the scan).

Component C: Significant negative correlations were found (a) between MPFC connectivity and SRS total score (x=6, y=48, z=28, r=0.91, $p_{FDR}<0.05$), and (b) between ACC connectivity and SRS total and autistic mannerisms subscale score (x=6, 38, 1, r=−0.85 and x=9, 38, −2, r=−0.93, respectively, $p_{FDR}<0.05$). All analyses were controlled for age and IQ; worse symptom severities were associated with decreased connectivity (Fig. 3).

Discussion

We investigated the integrity of FC within sub-networks of resting-state default mode areas in high-functioning patients with ASDs compared to matched healthy controls using ICA of relatively straightforward and short resting fMRI scans. Group ICA of fMRI data identifies components, each comprised of several brain regions with synchronous BOLD time courses. The regions in each component therefore have strong FC and can be considered as a specific neural network (for review see Calhoun et al., 2009). Of the 10 meaningful brain components we identified by ICA, 3 included brain regions most often associated with DMN (e.g. Broyd et al., 2009; Buckner et al., 2008; McKiernan et al., 2003; Raichle et al., 2001). *Component A* included all DMN areas, but mostly the PCC/PrC and bilateral IPL, *Component B* included mainly the PrC, and *Component C* included MPFC and ACC with a small cluster at the PCC. These 3 DM-SNs were previously identified in other ICA studies of resting state and cognitive fMRI studies in both non-clinical samples and schizophrenia patients (e.g. Assaf et al., 2009; Calhoun et al., 2008a; Damoiseaux et al., 2006; Esposito et al., 2006; Garrity et al., 2007; Jafri et al., 2008; Kim et al., 2009; Stevens et al., 2009). The heterogeneity of connectivity among regions indicates that spatiotemporal patterns of the MPFC/ACC and PrC are sufficiently different from the rest of the DMN (i.e. PCC and IPL); as such, they are identified by ICA as different components. Separation of DMN into posterior and anterior regions (corresponding to our components A and C) is the most consistent result in the above studies (Calhoun et al., 2008a; Damoiseaux et al., 2006; Esposito et al., 2006; Kim et al., 2009; Stevens et al., 2009). Working memory task load differentially influences these regions' temporal and spatial modulation (Esposito et al., 2006) and posterior regions show less activity modulation during resting scans (Damoiseaux

et al., 2006). To our knowledge, no study has investigated the temporospatial modulation of the PrC component, although its activity manifests task-related decreases (Calhoun et al., 2008a). Our results support the idea that the DMN has multiple interacting hubs or subsystems (Buckner et al., 2008).

Although all 3 DM-SNs were evident in both ASD and HC, direct group comparisons showed decreased connectivity strength in precuneus in component A and MPFC/ACC in component C (each with other brain areas in the corresponding component) in patients. There was no group difference in the connectivity of component B, representing local PrC FC. In addition, the connectivity integrity of different DMN areas negatively correlated with specific measures of patients' symptoms. Thus, decreased connectivity between DMN regions (a brain network associated with social cognitive functions impaired in individuals with ASD, see below) might underlie specific deficits in these patients, supporting the under-connectivity hypothesis of ASD (Just et al., 2004).

Our results mostly agree with other fMRI studies of DMN in ASD, generally showing decreased long-range (and not local) FC or activation of this network (Cherkassky et al., 2006; Kennedy and Courchesne, 2008a,b; Kennedy et al., 2006; Monk et al., 2009), although the impaired regions identified by these studies do not always overlap with ours. Methodological differences make direct comparisons between results somewhat challenging. Most previous studies used a task induced deactivation (TID) method in fMRI scans of cognitive tasks to explore the DMN (Cherkassky et al., 2006; Kennedy and Courchesne, 2008a; Kennedy et al., 2006). Of those, Kennedy and Courchesne (2008a) and Kennedy et al. (2006) linked ASD to abnormal deactivation of the DMN, but did not examine FC. Cherkassky et al. (2006), although not finding similar reduced TID, reported decreased connectivity between the ACC and precuneus in patients using a formal DMN connectivity analysis after combining data from different cognitive tasks. It is difficult to conclude whether group differences in these studies represent true abnormal DMN activity/ connectivity, or if they are driven by abnormal task-related performance (McKiernan et al., 2003).

In recent studies, Kennedy and Courchesne (2008b) and Monk et al. (2009) used resting fMRI scans similar to ours in individuals with ASD to explore FC among DMN brain regions, but reported conflicting results. Kennedy and Courchesne (2008b) found reduced connectivity in patients in the MPFC and left angular gyrus, but not in PCC/PrC. Monk et al. (2009) demonstrated *decreased* connectivity between PCC and frontal regions and *increased* connectivity between PCC and temporal regions. Importantly, these studies explored connectivity integrity by calculating correlations between time courses of pre-defined ROIs based on a previous study of DMN in healthy participants (Fox et al., 2005). This method could potentially bias results to specific areas while missing others. Conversely, ICA requires no *a priori* hypotheses regarding ROIs. Note that although we used a DMN mask to identify the most appropriate components, this procedure did not limit the ICA results to the regions included in this mask. Instead, this approach merely permitted us to empirically quantify how strongly any given component resembles the proposed structure of the DMN to choose what networks to examine. Since we used data from patients and controls to identify DM-SNs, and group differences were assessed by second-level analyses, our results are not biased by areas selected based on healthy participants data only.

Our results also show an association between connectivity strength of DMN regions and characteristic social, communication and behavioral deficits in patients. Areas in the PrC showed negative correlations with ADOS Total, Social and Communication scores (component B) while areas in the MPFC/ACC negatively correlated with SRS total score and the social mannerism subscale scores (component C). For all these correlations,

decreased functional connectivity was associated with more severe symptoms. The SRS is a parental report that assesses several dimensions of social, communication and repetitive/ stereotypic behaviors in ASDs. The Autistic Mannerisms subscale specifically measures stereotypical behaviors and highly restricted interests that characterize patients, including obsessive behaviors and thoughts (Constantino and Gruber, 2005). The ADOS is an observational tool, designed to elucidate and evaluate social and communication deficits specifically related to ASDs. Although SRS and ADOS scores are reported to correlate positively (Charman et al., 2007), they probably represent somewhat different aspects of patients' impairments. The SRS mannerism subscale in particular captures behavioral aspects not incorporated into the ADOS algorithm. Importantly, the association of the SRS with ACC FC corresponds to the documented involvement of the ACC in the pathopysiology of obsessive-compulsive disorder (for review see Maia et al., 2008; Rotge et al., 2009), suggesting that these symptoms in patients with ASD might have similar underlying neural cause (Hollander et al., 2009). On the other hand, the correlation between ADOS scores and the PrC FC corresponds to this region known involvement in high social cognitive processes, such as self-referential thinking (e.g. Cavanna and Trimble, 2006; Wolf et al., 2010) and ToM, which are known to be impaired in patients with ASD (Baron-Cohen, 1995; Frith and Frith, 2003; Hill and Frith, 2003). Related to our results in this region, Rojas et al. (2006) found negative correlation between PrC (among other regions) gray matter volume and ADI Social and Communication total score (although they did not find similar correlation with ADOS scores), further emphasizing the relationship between the PrC and social and communication deficits in patients with ASD.

While our correlation analysis results support an under-connec-tivity hypothesis of autism (Just et al., 2004), they are not in full agreement with other reports. To our knowledge only 3 studies to date have evaluated the correlations between FC and symptoms severity in ASD, two measured FC during cognitive tasks (Just et al., 2007; Kleinhans et al., 2008) and the third measured FC during a resting fMRI scan (Monk et al., 2009). Just et al. (2007) showed that frontal-parietal FC negatively correlated with ADOS total scores during an executive task. Using face processing task, Kleinhans et al. (2008) showed that FFA-amygdala FC negatively correlated with social impairments measured by ADI, but FFA-right IFG FC positively correlated with ADOS social impairments. Finally, Monk et al. (2009) showed negative correlations between social impairments (measured by ADI) and the FC between the PCC and MPFC, but positive correlations between restricted and repetitive behaviors and FC between PCC and parahippocampal region during resting scans similar to ours. Differences in results might arise from the methods used to measure FC (i.e. task vs. resting-state scans; ICA vs. voxel-based correlations) and symptom severity. Importantly, Components A–C depicted in our study did not include hippocampal/parahippo-campal regions, which have been suggested by some studies to be part of the DMN (for review see Buckner et al., 2008) and showed impaired connectivity in patients with ASD (Monk et al., 2009), and therefore we could not assess their connectivity to other DMN regions. Moreover, while the ADOS and SRS assess current symptoms the ADI assesses the most abnormal lifetime symptoms, also possibly contributing to seeming contradictions among existing results from different studies.

While DMN functions are still a matter of debate, a leading hypothesis suggests that the “resting brain” is engaged in self-referential mental representation and other high order social cognitive processes, such as ToM (for reviews see Broyd et al., 2009; Buckner et al., 2008), since although it deactivates during most cognitive tasks, it activates during tasks involving these processes. Thus, investigating the DMN FC from resting scans can potentially approximate FC of brain networks related to social cognition, allowing us to investigate brain networks hypothesized to be impaired in individuals with ASD (Baron-Cohen, 1995; Frith and Frith, 2003; Hill and Frith, 2003) without highly demanding

cognitive tasks (Franco et al., 2009; Pearlson and Calhoun, 2009). Importantly, this suggested functional significance of the DMN has been challenged by observations of its activity in unconscious states in both humans and monkeys (e.g. Boly et al., 2008; Horovitz et al., 2008; Vincent et al., 2007), implying that DMN activity might be related to intrinsic brain functional organization. Notably, these latter studies explored this activity in the "classic" DMN (mostly in PCC/PrC and IPL) but not in DM-SNs, such as the MPFC. Nevertheless, we do not argue that DM-SNs are exclusively involved in higher-order social processes. Rather we speculate that these sub-networks show coherent fluctuations during rest in different levels of consciousness and during social cognitive tasks, much like other brain networks, such as somatomotor and visual circuits (e.g. Vincent et al., 2007). Higher-order social cognitive processes are hypothesized to be impaired in patients with ASD and to underlie core social and communication clinical deficits (Baron-Cohen, 1995; Frith and Frith, 2003; Hill and Frith, 2003) and therefore it is logical to investigate patient DM-SNs activity and connectivity. Our results add to the growing evidence that regional DMN under-connectivity may underlie the etio-pathology of patients' clinical deficits. Furthermore, our findings suggest that assessing FC of fMRI data collected during a simple resting scan could serve as a biological marker for treatments designed to target specific deficits.

Limitations of the current study include that 8 of the 15 patients were medicated (data missing for 2 patients), making it difficult to determine whether some of our findings were secondary to possible effects of medication on FC. However, our analyses confirmed that the same group differences are evident when examining unmediated patients only and that medicated and unmediated patients showed no connectivity differences. In addition, as can be seen in Fig. 3, none of the 2 patients groups is driving the correlation of FC with symptoms severity. Albeit preliminary due to small sample size, these results suggest that connectivity impairments in patients with ASD are primarily due to their baseline illness and not drug treatment. Second, although resting-state fMRI's major advantage is its relative simplicity and lack of potential performance confounds, this can be also viewed as a disadvantage, since participants are not monitored through the scan and no cognitive data exists to interpret the results. For example, we did not objectively verify that participants had not fallen asleep during the scan. However, all patients responded to the MR technologist at the beginning and end of the scan and no subject indicated that they slept during the resting scan. It is also possible that group differences are due to different anxiety/arousal levels, which are more prevalent in individuals with ASD (Davism et al., 2008); however, we did not assess anxiety. Third, we did not evaluate mutual casual interactions among different ICA DM-SN components and their potential impairments in patients with ASD (Assaf et al., 2009;Jafri et al., 2008). Finally, our sample included only high-functioning patients with ASD, limiting generalizability. Given the simplicity of resting scans, applying our methods to lower-functioning patients is an obtainable goal.

In summary, using brief resting fMRI scans and ICA, we have shown that although high-functioning patients with ASD have similar DM-SNs to healthy controls, they have decreased connectivity in the MPFC/ACC and PrC regions. Strength of connectivity in these regions also negatively correlated with the severity of patients' social and communication deficits. These results are in accord with an ASD under-connectivity hypothesis, which suggests that a general decrease in cortico-cortical functional connectivity underlies patients' behavioral and cognitive impairments. Resting fMRI scans and ICA as a data analysis method provide us with the tools to probe this network easily without a cognitive task (that patients might find difficult to understand and/or perform) opening the way to explore functional connectivity in younger and low-functioning patients with ASD as well. If our results generalize to these patients, DMN connectivity promises to be a useful imaging biological marker and treatment target of ASD.

Supplementary Material

Refer to Web version on PubMed Central for supplementary material.

Acknowledgments

This work was supported by grants from Autism Speaks and Hartford Hospital (PI: M. Assaf), and from NIH 2R01 EB000840 (PI: V. D. Calhoun). Parts of these data were presented in the 2009 IMFAR annual meeting, Chicago, IL, May, 2009.

References

Assaf M, Jagannathan K, Calhoun V, Kraut M, Hart J Jr, Pearlson G. Temporal sequence of hemispheric network activation during semantic processing: a functional network connectivity analysis. Brain Cogn. 2009; 70:238–246. [PubMed: 19307050]

Baron-Cohen, S. Cambridge, Mass: MIT Press; 1995. Mindblindness : an essay on autism and theory of mind.

Baron-Cohen S, Ring HA, Wheelwright S, Bullmore ET, Brammer MJ, Simmons A, Williams SC. Social intelligence in the normal and autistic brain: an fMRI study. Eur. J. Neuro sci. 1999; 11:1891–1898.

Beckmann CF, DeLuca M, Devlin JT, Smith SM. Investigations into resting-state connectivity using independent component analysis. Philos. Trans. R. Soc. Lond. B Biol Sci. 2005; 360:1001–1013. [PubMed: 16087444]

Bell AJ, Sejnowski TJ. An information maximization approach to blind separation and blind deconvolution. Neural Comput. 1995; 7:1129–1159. [PubMed: 7584893]

Boly M, Phillips C, Tshibanda L, Vanhaudenhuyse A, Schabus M, Dang Vu TT, Moonen G, Hustinx R, Maquet P, Laureys S. Intrinsic brain activity in altered states of consciousness: how conscious is the default mode of brain function? Ann. N. Y. Acad Sci. 2008; 1129:119–129. [PubMed: 18591474]

Broyd SJ, Demanuele C, Debener S, Helps SK, James CJ, Sonuga Barke EJ. Default-mode brain dysfunction in mental disorders: a systematic review. Neurosci. Biobehav Rev. 2009; 33:279–296. [PubMed: 18824195]

Buckner RL, Andrews-Hanna JR, Schacter DL. The brain's default network: anatomy, function, and relevance to disease. Ann. N. Y. Acad Sci. 2008; 1124:1–38. [PubMed: 18400922]

Calhoun VD, Adali T, Pearlson GD, Pekar JJ. A method for making group inferences from functional MRI data using independent component analysis. Hum Brain Mapp. 2001a; 14:140–151. [PubMed: 11559959]

Calhoun VD, Adali T, Pearlson GD, Pekar JJ. Spatial and temporal independent component analysis of functional MRI data containing a pair of task-related waveforms. Hum Brain Mapp. 2001b; 13:43–53. [PubMed: 11284046]

Calhoun VD, Kiehl KA, Pearlson GD. Modulation of temporally coherent brain networks estimated using ICA at rest and during cognitive tasks. Hum Brain Mapp. 2008a; 29:828–838. [PubMed: 18438867]

Calhoun VD, Maciejewski PK, Pearlson GD, Kiehl KA. Temporal lobe and “default” hemodynamic brain modes discriminate between schizophrenia and bipolar disorder. Hum Brain Mapp. 2008b; 29:1265–1275. [PubMed: 17894392]

Calhoun VD, Liu J, Adali T. A review of group ICA for fMRI data and ICA for joint inference of imaging, genetic, and ERP data. Neuroimage. 2009; 45:S163–S172. [PubMed: 19059344]

Castelli F, Frith C, Happe F, Frith U. Autism, Asperger syndrome and brain mechanisms for the attribution of mental states to animated shapes. Brain. 2002; 125:1839–1849. [PubMed: 12135974]

Cavanna AE, Trimble MR. The precuneus: a review of its functional anatomy and behavioural correlates. Brain. 2006; 129:564–583. [PubMed: 16399806]

Charman T, Baird G, Simonoff E, Loucas T, Chandler S, Meldrum D, Pickles A. Efficacy of three screening instruments in the identification of autistic-spectrum disorders. Br. J Psychiatry. 2007; 191:554–559. [PubMed: 18055961]

Cherkassky VL, Kana RK, Keller TA, Just MA. Functional connectivity in a baseline resting-state network in autism. Neuroreport. 2006; 17:1687–1690. [PubMed: 17047454]

Constantino, JN.; Gruber, CP. Western Psychological Services. Los Angeles, California: 2005. Social Responsiveness Scale (SRS).

Damoiseaux JS, Rombouts SA, Barkhof F, Scheltens P, Stam CJ, Smith SM, Beckmann CF. Consistent resting-state networks across healthy subjects. Proc. Natl. Acad. Sci. U. S. A. 2006; 103:13848–13853. [PubMed: 16945915]

Davism E, Saeed SA, Antonacci DJ. Anxiety disorders in persons with developmental disabilities: empirically informed diagnosis and treatment. Reviews literature on anxiety disorders in DD population with practical take-home messages for the clinician. Psychiatr Q. 2008; 79:249–263. [PubMed: 18726156]

De Luca M, Beckmann CF, De Stefano N, Matthews PM, Smith SM. fMRI resting state networks define distinct modes of long-distance interactions in the human brain. Neuroimage. 2006; 29:1359–1367. [PubMed: 16260155]

Esposito F, Bertolino A, Scarabino T, Latorre V, Blasi G, Popolizio T, Tedeschi G, Cirillo S, Goebel R, Di Salle F. Independent component model of the default-mode brain function: Assessing the impact of active thinking. Brain Res Bull. 2006; 70:263–269. [PubMed: 17027761]

Fox MD, Snyder AZ, Vincent JL, Corbetta M, Van Essen DC, Raichle ME. The human brain is intrinsically organized into dynamic, anticorrelated functional networks. Proc. Natl. Acad. Sci. U. S. A. 2005; 102:9673–9678. [PubMed: 15976020]

Franco AR, Pritchard A, Calhoun VD, Mayer AR. Interrater and intermethod reliability of default mode network selection. Hum. Brain Mapp. 2009; 30:2293–2303. [PubMed: 19206103]

Friston KJ, Frith CD, Liddle PF, Frackowiak RS. Functional connectivity: the principal-component analysis of large (PET) data sets. J. Cereb Blood Flow Metab. 1993; 13:5–14. [PubMed: 8417010]

Friston KJ, Ashburner J, Frith CD, Poline J-B, Heather JD, Frackowiak RSJ. Spatial registration and normalization of images. Hum. Brain Mapp. 1995; 2:165–189.

Frith U, Frith CD. Development and neurophysiology of mentalizing. Philos. Trans. R. Soc. Lond. B Biol Sci. 2003; 358:459–473. [PubMed: 12689373]

Garrity AG, Pearlson GD, McKiernan K, Lloyd D, Kiehl KA, Calhoun VD. Aberrant “default mode” functional connectivity in schizophrenia. Am. J Psychiatry. 2007; 164:450–457. [PubMed: 17329470]

Happé F, Ehlers S, Fletcher P, Frith U, Johansson M, Gillberg C, Dolan R, Frackowiak R, Frith C. ‘Theory of mind' in the brain. Evidence from a PET scan study of Asperger syndrome. Neuroreport. 1996; 8:197–201. [PubMed: 9051780]

Hill EL, Frith U. Understanding autism: insights from mind and brain. Philos. Trans. R. Soc. Lond. B Biol Sci. 2009; 358:281–289. [PubMed: 12639326]

Hollander E, Kim S, Braun A, Simeon D, Zohar J. Cross-cutting issues and future directions for the OCD spectrum. Psychiatry Res. 2009; 170:3–6. [PubMed: 19811839]

Horovitz SG, Fukunaga M, de Zwart JA, van Gelderen P, Fulton SC, Balkin TJ, Duyn JH. Low frequency BOLD fluctuations during resting wakefulness and light sleep: a simultaneous EEG-fMRI study. Hum. Brain Mapp. 2008; 29:671–682. [PubMed: 17598166]

Jafri MJ, Pearlson GD, Stevens M, Calhoun VD. A method for functional network connectivity among spatially independent resting-state components in schizophrenia. Neuroimage. 2008; 39:1666–1681. [PubMed: 18082428]

Just MA, Cherkassky VL, Keller TA, Minshew NJ. Cortical activation and synchronization during sentence comprehension in high-functioning autism: evidence of underconnectivity. Brain. 2004; 127:1811–1821. [PubMed: 15215213]

Just MA, Cherkassky VL, Keller TA, Kana RK, Minshew NJ. Functional and anatomical cortical underconnectivity in autism: evidence from an FMRI study of an executive function task and corpus callosum morphometry. Cereb Cortex. 2007; 17:951–961. [PubMed: 16772313]

Kana RK, Keller TA, Cherkassky VL, Minshew NJ, Just MA. Sentence comprehension in autism: thinking in pictures with decreased functional connectivity. Brain. 2006; 129:2484–2493. [PubMed: 16835247]

Kana RK, Keller TA, Minshew NJ, Just MA. Inhibitory control in high-functioning autism: decreased activation and underconnectivity in inhibition networks. Biol Psychiatry. 2007; 62:198–206. [PubMed: 17137558]

Kana RK, Keller TA, Cherkassky VL, Minshew NJ, M.A.J. Atypical frontal- posterior synchronization of Theory of Mind regions in autism during mental state attribution. Soc Neuro sci. 2009; 4:135–152.

Kennedy DP, Courchesne E. Functional abnormalities of the default network during self- and other-reflection in autism. Soc. Cogn. Affect Neuro sci. 2008a; 3:177–190.

Kennedy DP, Courchesne E. The intrinsic functional organization of the brain is altered in autism. Neuroimage. 2008b; 39:1877–1885. [PubMed: 18083565]

Kennedy DP, Redcay E, Courchesne E. Failing to deactivate: resting functional abnormalities in autism. Proc. Natl. Acad. Sci. U. S. A. 2006; 103:8275–8280. [PubMed: 16702548]

Kim DI, Manoach DS, Mathalon DH, Turner JA, Mannell M, Brown GG, Ford JM, Gollub RL, White T, Wible C, Belger A, Bockholt HJ, Clark VP, Lauriello J, O'Leary D, Mueller BA, Lim KO, Andreasen N, Potkin SG, Calhoun VD. Dysregulation of working memory and default-mode networks in schizophrenia using independent component analysis, an fBIRN and MCIC study. Hum. Brain Mapp. 2009; 30(11):3795–3811. [PubMed: 19434601]

Kleinhans NM, Richards T, Sterling L, Stegbauer KC, Mahurin R, Johnson LC, Greenson J, Dawson G, Aylward E. Abnormal functional connectivity in autism spectrum disorders during face processing. Brain. 2008; 131:1000–1012. [PubMed: 18234695]

Koshino H, Carpenter PA, Minshew NJ, Cherkassky VL, Keller TA, Just MA. Functional connectivity in an fMRI working memory task in high-functioning autism. Neuroimage. 2005; 24:810–821. [PubMed: 15652316]

Koshino H, Kana RK, Keller TA, Cherkassky VL, Minshew NJ, Just MA. fMRI investigation of working memory for faces in autism: visual coding and under-connectivity with frontal areas. Cereb Cortex. 2008; 18:289–300. [PubMed: 17517680]

Lee PS, Yerys BE, Della Rosa A, Foss-Feig J, Barnes KA, James JD, Vanmeter J, Vaidya CJ, Gaillard WD, Kenworthy LE. Functional Connectivity of the Inferior Frontal Cortex Changes with Age in Children with Autism Spectrum Disorders: A fcMRI Study of Response Inhibition. Cereb Cortex. 2008; 19:1787–1794. [PubMed: 19068486]

Li YO, Adali T, Calhoun VD. Estimating the number of independent components for functional magnetic resonance imaging data. Hum. Brain Mapp. 2007; 28:1251–1266. [PubMed: 17274023]

Lord C, Rutter M, Le Couteur A. Autism Diagnostic Interview-Revised: a revised version of a diagnostic interview for caregivers of individuals with possible pervasive developmental disorders. J. Autism Dev Disord. 1994; 24:659–685. [PubMed: 7814313]

Lord C, Risi S, Lambrecht L, Cook EH Jr, Leventhal BL, DiLavore PC, Pickles A, Rutter M. The autism diagnostic observation schedule-generic: a standard measure of social and communication deficits associated with the spectrum of autism. J. Autism Dev Disord. 2000; 30:205–223. [PubMed: 11055457]

Maia TV, Cooney RE, Peterson BS. The neural bases of obsessive-compulsive disorder in children and adults. Dev Psychopathol. 2008; 20:1251–1283. [PubMed: 18838041]

Maldjian JA, Laurienti PJ, Kraft RA, Burdette JH. An automated method for neuroanatomic and cytoarchitectonic atlas-based interrogation of fMRI data sets. Neuroimage. 2003; 19:1233–1239. [PubMed: 12880848]

Mason RA, Williams DL, Kana RK, Minshew N, Just MA. Theory of Mind disruption and recruitment of the right hemisphere during narrative comprehension in autism. Neuropsychologia. 2008; 46:269–280. [PubMed: 17869314]

McKeown MJ, Sejnowski TJ. Independent component analysis of fMRI data: examining the assumptions. Hum. Brain Mapp. 1998; 6:368–372. [PubMed: 9788074]

McKiernan KA, Kaufman JN, Kucera-Thompson J, Binder JR. A parametric manipulation of factors affecting task-induced deactivation in functional neuroi-maging. J. Cogn Neurosci. 2003; 15:394–408. [PubMed: 12729491]

Mizuno A, Villalobos ME, Davies MM, Dahl BC, Muller RA. Partially enhanced thalamocortical functional connectivity in autism. Brain Res. 2006; 1104:160–174. [PubMed: 16828063]

Monk CS, Peltier SJ, Wiggins JL, Weng SJ, Carrasco M, Risi S, Lord C. Abnormalities of intrinsic functional connectivity in autism spectrum disorders. Neuroimage. 2009; 47:764–772. [PubMed: 19409498]

Mostofsky SH, Powell SK, Simmonds DJ, Goldberg MC, Caffo B, Pekar JJ. Decreased connectivity and cerebellar activity in autism during motor task performance. Brain. 2009; 132:2413–2425. [PubMed: 19389870]

Pearlson GD, Calhoun VD. Convergent approaches for defining functional imaging endophenotypes in schizophrenia. Front. Hum Neurosci. 2009; 3:37. [PubMed: 19956400]

Piggot J, Kwon H, Mobbs D, Blasey C, Lotspeich L, Menon V, Bookheimer S, Reiss AL. Emotional attribution in high-functioning individuals with autistic spectrum disorder: a functional imaging study. J. Am. Acad. Child Adolesc Psychiatry. 2004; 43:473–480.

Raichle ME, MacLeod AM, Snyder AZ, Powers WJ, Gusnard DA, Shulman GL. A default mode of brain function. Proc. Natl. Acad. Sci. U. S. A. 2001; 98:676–682. [PubMed: 11209064]

Rojas DC, Peterson E, Winterrowd E, Reite ML, Rogers SJ, Tregellas JR. Regional gray matter volumetric changes in autism associated with social and repetitive behavior symptoms. BMC Psychiatry. 2006; 6:56. [PubMed: 17166273]

Rotge JY, Guehl D, Dilharreguy B, Tignol J, Bioulac B, Allard M, Burbaud P, Aouizerate B. Meta-analysis of brain volume changes in obsessive- compulsive disorder. Biol Psychiatry. 2009; 65:75–83. [PubMed: 18718575]

Rutter, M.; Bailey, A.; Lord, C. Western Psychological Services. Los Angeles, California: 2003. Social Communication Questionnaire–WPS edition.

Solomon M, Ozonoff SJ, Ursu S, Ravizza S, Cummings N, Ly S, Carter CS. The neural substrates of cognitive control deficits in autism spectrum disorders. Neuropsychologia. 2009; 47:2515–2526. [PubMed: 19410583]

Stevens MC, Kiehl KA, Pearlson G, Calhoun VD. Functional neural circuits for mental timekeeping. Hum. Brain Mapp. 2007; 28:394–408. [PubMed: 16944489]

Stevens MC, Pearlson GD, Calhoun VD. Changes in the interaction of resting-state neural networks from adolescence to adulthood. Hum. Brain Mapp. 2009; 30:2356–2366. [PubMed: 19172655]

Talairach, J.; Tournoux, P. Thieme. New York: 1988. A co-planar stereotaxic atlas of a human brain.

Turner KC, Frost L, Linsenbardt D, McIlroy JR, Muller RA. Atypically diffuse functional connectivity between caudate nuclei and cerebral cortex in autism. Behav. Brain Funct. 2006; 2:34. [PubMed: 17042953]

Uddin LQ, Kelly AM, Biswal BB, Xavier Castellanos F, Milham MP. Functional connectivity of default mode network components: correlation, antic-orrelation, and causality. Hum. Brain Mapp. 2009; 30:625–637. [PubMed: 18219617]

van de Ven VG, Formisano E, Prvulovic D, Roeder CH, Linden DE. Functional connectivity as revealed by spatial independent component analysis of fMRI measurements during rest. Hum. Brain Mapp. 2004; 22:165–178. [PubMed: 15195284]

Vincent JL, Patel GH, Fox MD, Snyder AZ, Baker JT, Van Essen DC, Zempel JM, Snyder LH, Corbetta M, Raichle ME. Intrinsic functional architecture in the anaesthetized monkey brain. Nature. 2007; 447:83–86. [PubMed: 17476267]

Wolf I, Dziobek I, Heekeren HR. Neural correlates of social cognition in naturalistic settings: a model-free analysis approach. Neuroimage. 2010; 49:894–904. [PubMed: 19733672]

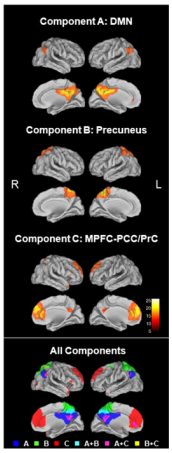

Fig. 1.

The upper panel depicts the 3 ICA components that represent the Default Mode sub-networks. These maps were identified by GIFT (http://icatb.sourceforge.net/, version 1.3e) using resting scans data from all 32 participants (patients and controls) and thresholded at $p < 0.05$ corrected for family-wise errors. The lower panel shows all 3 components concurrently.

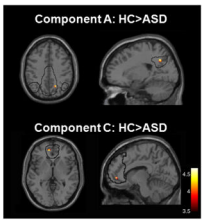

Fig. 2.

Group differences in the Default Mode sub-networks. Only the PrC in Component A and MPFC in component C showed significant group differences, such that patients had decreased strength of connectivity. Each map is masked with the corresponding component mask generated from all participants (black outline, see Fig. 1) and threshold at $p_{FDR} < 0.05$.

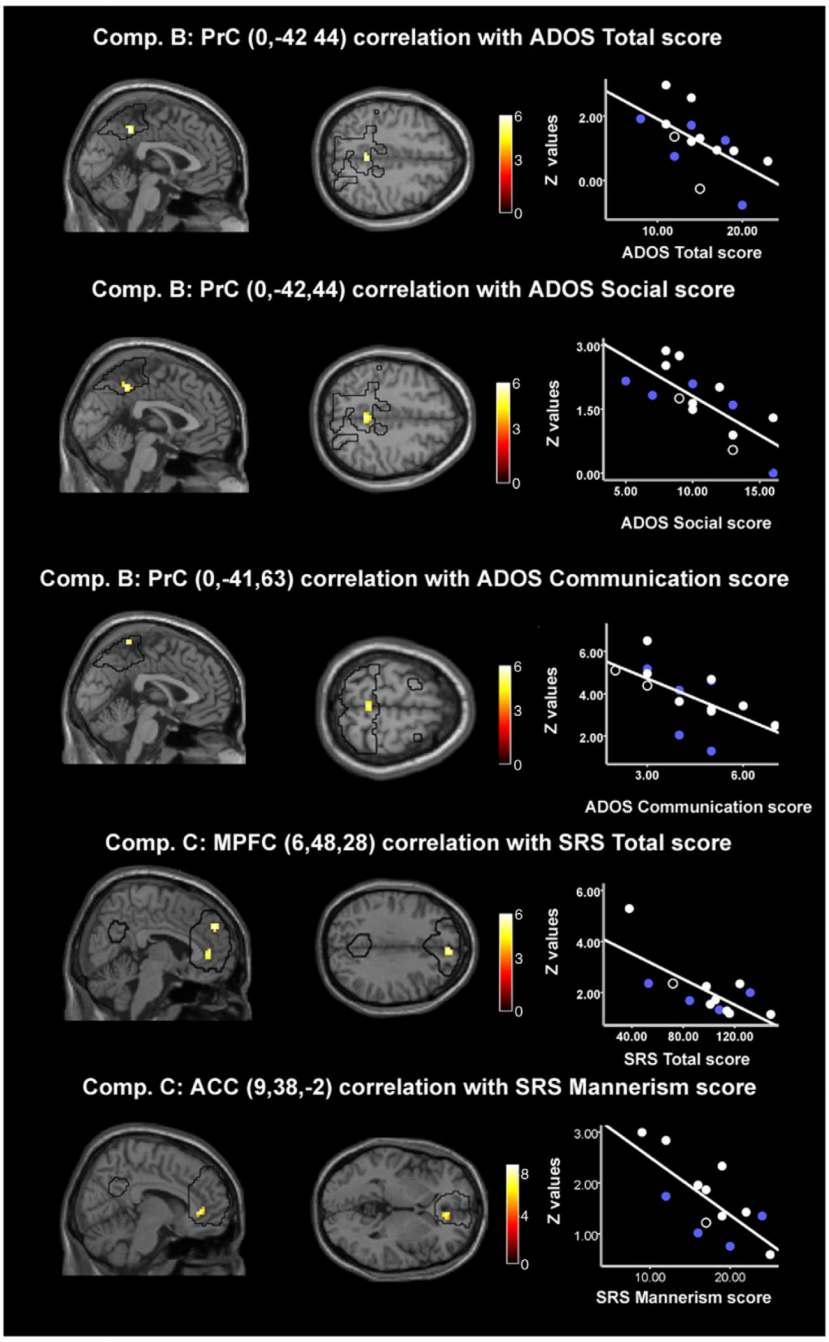

Fig. 3.

Correlations between the functional connectivity strength of the Default Mode sub-networks and ADOS and SRS scores in patients with ASD. Patients receiving treatment at the time of the scan are depicted as filled white circles, patients without drug treatment at the time of the scan are depicted as blue circles, and patients with unknown treatment status are shown as unfilled white circles. Each map is masked with the corresponding component mask generated from all participants (black outline, see Fig. 1) and threshold at $p_{FDR} < 0.05$. Note that the graph for the ACC cluster (shown in the two lower panels) correlation with SRS total scores is not displayed. Also, no significant correlation was found for component (comp.) A. ACC, anterior cingulate cortex; MPFC, medial prefrontal cortex; PrC, precuneus.

Table 1

Demographic and symptoms assessment information. (Data represents average scores ± standard deviation).

	ASD (n=15)	**HC (n=15)**	**Statistics**	***p***
Age (years) (range)	15.7±3.0 (11–20)	17.1 ±3.6 (10–23)	t(28) = –1.1	n.s.
Gender (M/F)	14/1	13/2	$\chi^2(1) = 0.4$	n.s.
Race (W/B/O)	14/0/1	10/3/2	$\chi^2(3) = 4.7$	n.s.
FSIQ (range)	113.3 ±15.0 (79–135)	117.1 ±16.9 (79–139)	t(28) = –0.7	n.s.
ADOS total (n = 15/14)	14.9 ±4.0	0.8 ±1.2	t(27) =12.7	<0.0001
ADOS communication (n = 15/14)	4.3 ±1.3	0.6 ±1.2	t(27) =7.6	<0.0001
ADOS social (n = 15/14)	10.6±3.2	0.1 ±0.4	t(27) =12.2	<0.0001
SRS Total (n = 13)	99.6 ±31.0	–		
SRS Social Awareness (n = 13)	11.5 ± 4.4	–		
SRS Social Cognition (n = 13)	16.8±6.8	–		
SRS Social Communication (n = 13)	31.5 ±11.8	–		
SRS Social Motivation (n = 13)	18.1 ±7.5	–		
SRS Social Mannerism (n=13)	17.0 ± 4.3	–		

Table 2

Brain regions identified in each of the Default Mode sub-networks (DM-SN) components. The table depicts regions' anatomic location, Talairach coordinates for peak activation voxel in each brain region, and *t* scores from random effects analyses across all participants (n=32; $p_{FWE}<0.05$) and for patients and controls (n=15 per group; $p_{FDR}<0.05$) separately.

Anatomic Location	All Participants (Fig. 1)				ASD Patients				Healthy Controls			
	Left Hemi.		Right Hemi.		Left Hemi.		Right Hemi.		Left Hemi.		Right Hemi.	
	TC	*t*	TC	*t*	TC	*t*	TC	*t*	TC	t	TC	*t*
Component A												
PCC (BA 23, 31, 30, 29)	−3,−45, 35	24.0	3, −45, 35	24.7	−6, −48, 25	25.8	6, −33, 29	17.2	−9, −42, 33	23.5	6, −45, 33	26.0
PrC (BA 7, 19, 31)	−3,−68, 34	24.7	9, −57, 30	21.4	−6, −68, 34	16.7	12, −71, 42	17.0	−6, −63, 28	25.7	12, −53, 38	20.2
IPL (BA 7, 39, 40)	−45, −62, 42	12.9	45, −62, 42	11.3	−45, −56, 44	9.9	−42, −62, 34	10.4	−50, −54, 33	10.0	−42, −62, 39	9.5
ACC (BA 24, 32)	−3, 44,−2	8.4	3, 41, 6	6.4	–3, 43, −5	8.7	3, 43, −5	5.0	−9, 35, −2	6.3	6, 44, 9	6.9
Component B												
PrC (BA 7, 19, 31)	−9, −58, 58	23.6	9, −58, 61	18.5	−21, −50, 55	19.0	9, −55, 61	12.7	−6, −58, 58	18.1	3, −52, 61	13.2
Postcentral G.	−12, −52, 63	23.1	12, −52, 66	24.0	−9, −52, 63	16.8	15, −52, 63	16.9	−12, −52, 63	14.1	12, −52, 66	16.0
Paracentral Lobule	−3, −44, 60	15.3	0, −41, 60	17.7	−3, 44, 60	10.0	3, 44, 60	11.3	−3, −41, 57	12.1	0, −38, 52	13.8
MiFG (BA 6)	−24, 3, 58	7.1	30, 6, 60	9.0	−24, 8, 47	5.7	24, 2, 47	5.2	−24, 6, 55	11.5	30, 11, 55	8.3
PCC (BA 31)	−12, −24, 37	8.5	3, −47, 41	7.4	−12, −27, 40	5.7	15, −30, 40	5.0	−15, −25, 34	8.9	6, −47, 41	6.2
Insula	−39,−12, −4	7.0			−39, −9, −5	6.3			−45, −14, 6	5.3		
SOG (BA 19)	−36, −77, 29	6.9			−39, −77, 29	5.0			−36, −83, 29	7.5		
Component C												
MFG/SFG (BA 6,8,9,10, 32)	−3, 57, 25	24.8	3, 51, 20	28.0	−6, 42, 15	35.1	3, 41, 12	25.5	−3, 59, 14	19.0	3, 51, 20	17.1
ACC (BA 24, 32)	−6, 47, 3	19.0	3, 47, −2	21.8	−9, 49, −2	13.2	6, 52, 0	15.4	−6, 49, −2	20.3	6, 47, −2	22.0
PCC/PrC (BA 23, 31)	−3, −51, 33	10.8	3, −51, 33	12.4	−3, −54, 30	7.7	3, −54, 30	8.9	9, −54, 30	8.5	6, −51, 33	9.4
IFG (BA 13, 45, 47)			36, 17, −13	8.5			48, 18, 5	7.7			30, 14, −11	6.8
MOG/SOG (BA 18, 19)			36, −87, 18	8.4			42, −84, 15	7.2			36, −86, 24	13.3
SPL (BA 7)			30, −52, 61	8.1			24, −52, 61	5.6			30, −49, 61	6.7
STG/TP (BA 38)	−45, 16, −26	7.3	45, 16, −29	7.6			53, 2, −23	7.5	−39, 16,−31	6.6	45, 13, −28	6.3
IPL (BA 38, 39, 40)	−56, −63, 28	7.5	53, −51, 33	7.3	−50, −68, 37	6.6	53, −48, 33	5.4	−56, −60, 31	4.7	56, −54, 25	7.7
Paracentral Lb. (BA 31)	−3, −15, 45	7.1	0, −12, 45	7.4	−3, −9, 47	7.2	0, −9, 45	5.2	−3, −24, 45	8.5	0, −21, 45	7.8
Precentral Gyrus	−33, −15, 56	7.0			−30, −18, 56	7.9						
Declive			33, −62, −15	6.9			18, −53,−12	7.7			33, −65, −14	4.7

Anatomic Location	All Participants (Fig. 1)				ASD Patients				Healthy Controls			
	Left Hemi.		Right Hemi.		Left Hemi.		Right Hemi.		Left Hemi.		Right Hemi.	
	TC	*t*	TC	*t*	TC	*t*	TC	*t*	TC	t	TC	*t*
Lentiform Nucleus	−15, 6, −5	6.8	18, 6, −3	6.6	−15, 6, −5	4.9			15, 6,−3	5.7	24, 12, 2	6.0

ACC, anterior cingulate cortex; BA, Brodmann's area; IFG, inferior frontal gyrus; IPL, inferior parietal lobule; MFG, medial frontal gyrus; MiFG, middle frontal gyrus; MOG, middle occipital gyrus; PCC, posterior cingulate cortex; PrC, precuneus; SFG, superior frontal gyrus; SOG, superior occipital gyrus; SPL, superior parietal lobule; STG, superior temporal gyrus; TC, Talairach coordinate; TP, temporal pole.